Gravitational Bose-Einstein Condensation in the Kinetic Regime

D. G. Levkov,[1,2,*] A. G. Panin,[1,2] and I. I. Tkachev[1,3]
[1]Institute for Nuclear Research of the Russian Academy of Sciences, Moscow 117312, Russia
[2]Moscow Institute of Physics and Technology, Dolgoprudny 141700, Russia
[3]Novosibirsk State University, Novosibirsk 630090, Russia

(Received 18 April 2018; revised manuscript received 11 August 2018; published 12 October 2018)

We study Bose-Einstein condensation and the formation of Bose stars in virialized dark matter halos and miniclusters by universal gravitational interactions. We prove that this phenomenon does occur and it is described by a kinetic equation. We give an expression for the condensation time. Our results suggest that Bose stars may form kinetically in mainstream dark matter models such as invisible QCD axions and fuzzy dark matter.

DOI: 10.1103/PhysRevLett.121.151301

Introduction.—Bose stars are lumps of Bose-Einstein condensates bound be self-gravity [1,2]. They can be made of condensed dark matter (DM) bosons—say, invisible QCD axions [3] or fuzzy DM [4]. That is why their physics, phenomenology, and observational signatures have remained in the focus of cosmological research for decades [5]; see the recent papers [6,7]. Unfortunately, the formation of Bose stars is still poorly understood, and many recent works have to assume their existence.

In this Letter, we study Bose-Einstein condensation in the virialized DM halos and miniclusters caused by universal gravitational interactions. We work at large occupation numbers, which is correct if the DM bosons are light. Notably, we consider the kinetic regime where the initial coherence length and period of the DM particles are close to the de Broglie values $(mv)^{-1}$ and $(mv^2)^{-1}$ and much smaller than the halo size R and condensation time τ_{gr},

$$mvR \gg 1, \qquad mv^2\tau_{gr} \gg 1. \tag{1}$$

We numerically solve microscopic equations for the ensemble of gravitating bosons in this case and find that Bose stars indeed form. We derive an expression for τ_{gr} and study the kinetics of the process.

To our knowledge, gravitational Bose-Einstein condensation in the kinetic regime has not been observed in simulations before. Old works considered only contact interactions between the DM bosons [8] which are nonuniversal and suppressed by quartic constants $\lambda \sim 10^{-50}$ [9] and 10^{-100} [10] in models of QCD axions and fuzzy DM (string axions). Our results show that in these cases gravitational condensation is *faster*: Although the Newton constant Gm^2 is tiny, its effect is enhanced by the collective interaction of large fluctuations in the boson gas at large distances; cf. [11].

On the other hand, all previous numerical studies of Bose star formation considered coherent initial configurations of the bosonic field—a Gaussian wave packet [12] or the Bose stars themselves [13,14]. A spectacular simulation of structure formation by wavelike (fuzzy) DM [13,15] started from a (almost) homogeneous Bose-Einstein condensate. In all these cases, the Bose stars form almost immediately [12,13] from the lowest-energy part of the initial condensate.

We consider an entirely different situation (1) when the DM bosons are virialized in the initial state. The closest study to ours was performed in Ref. [16], but the kinetic regime was not achieved there due to computational limitations. Note that we do not consider the scenario of Ref. [11], where axions form a cosmological condensate at the radiation-dominated stage; cf. [17]. Indeed, at realignment, the momenta of such axions are comparable to the Hubble scale, and Eq. (1) is violated.

The birth of the Bose star.—Consider N nonrelativistic gravitationally interacting bosons in a periodic box of size L. At large occupation numbers, this system is described by a random classical field $\psi(t,\boldsymbol{x})$ [8,18] evolving in its own gravitational potential $U(t,\boldsymbol{x})$:

$$i\partial_t\psi = -\Delta\psi/2m + mU\psi,$$
$$\Delta U = 4\pi Gm(|\psi|^2 - n), \tag{2}$$

where the mean particle density $n \equiv N/L^3$ is subtracted in the second line for consistency [15]. Notably, Eqs. (2) simplify in dimensionless variables: Substitutions $\boldsymbol{x} = \tilde{\boldsymbol{x}}/mv_0$, $t = \tilde{t}/mv_0^2$, $U = v_0^2\tilde{U}$, and $\psi = v_0^2\tilde{\psi}\sqrt{m/G}$ exclude parameters m and G from the equations and reference velocity v_0 from the initial conditions. The rescaled particle number is $\tilde{N} \equiv \int d^3\tilde{\boldsymbol{x}}|\tilde{\psi}|^2 = Gm^2N/v_0$.

We fix the initial conditions in momentum space. A representative class of them describes Gaussian-distributed bosons, $|\tilde{\psi}_{\tilde{\boldsymbol{p}}}|^2 = 8\pi^{3/2}\tilde{N}e^{-\tilde{\boldsymbol{p}}^2}$, with random phases $\arg\tilde{\psi}_{\tilde{\boldsymbol{p}}}$, where $\tilde{\boldsymbol{p}} \equiv \boldsymbol{p}/mv_0$. Fourier-transforming $\tilde{\psi}_{\tilde{\boldsymbol{p}}}$, we obtain an isotropic and homogeneous initial configuration $\tilde{\psi}(0,\tilde{\boldsymbol{x}})$ with a minimal coherence length in Fig. 1(a). Then we

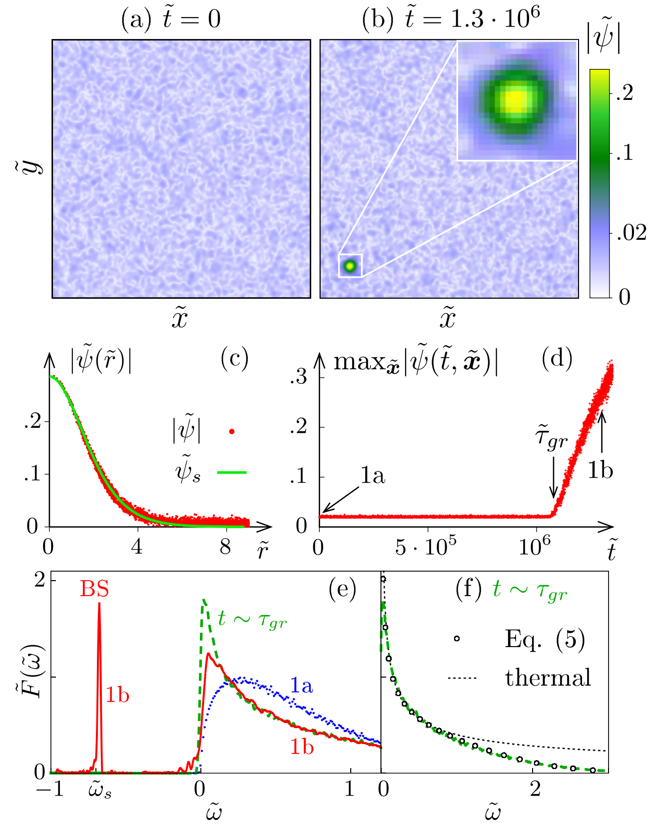

FIG. 1. Formation of a Bose star from a random field with initial distribution $|\tilde{\psi}_{\tilde{\boldsymbol{p}}}|^2 \propto e^{-\tilde{\boldsymbol{p}}^2}$ and total mass $\tilde{N} = 50$ in the box $0 \leq \tilde{x}, \tilde{y}, \tilde{z} < 125$. These values correspond to the center of the axion minicluster with $M_c \sim 10^{-13}\, M_\odot$ and $\Phi \sim 2.7$ in the discussion at the end of this Letter. (a),(b) Sections $\tilde{z} = \text{const}$ of the solution $|\tilde{\psi}(\tilde{t}, \tilde{\boldsymbol{x}})|$ at (a) $\tilde{t} = 0$ and (b) $\tilde{t} > \tilde{\tau}_{gr} \approx 1.08 \times 10^6$. (c) Radial profile $|\tilde{\psi}(\tilde{r})|$ of the object in (b) (points) compared to the Bose star $\tilde{\psi}_s(\tilde{r})$ with $\tilde{\omega}_s \approx -0.7$ (line). (d) Maximum of $|\tilde{\psi}(\tilde{\boldsymbol{x}})|$ over the box as a function of time. (e) Spectra (3) at times of (a) and (b) and at the eve of Bose star nucleation, $\tilde{t} = 1.05 \times 10^6 \sim \tilde{\tau}_{gr}$. (f) The spectrum at $t \sim \tau_{gr}$ (dashed line) versus the solution of Eq. (5) (circles) and thermal law $\tilde{F} \propto \tilde{\omega}^{-1/2}$ (dots).

numerically evolve Eqs. (2) using an exceptionally stable 3D algorithm; see Supplemental Material, Sec. S2 and movie [19], and Refs. [20,21]. Apart from the erratic motion of ψ peaks and depths, nothing happens for a long time $t < \tau_{gr}$, where $\tilde{\tau}_{gr} \sim 10^6$ for the solution in Fig. 1. Then a coherent, compact, and spherically symmetric object appears at $t > \tau_{gr}$; see Fig. 1(b). With time, the object grows in mass and moves in a Brownian way due to the interaction with the fluctuating environment.

To explain what happens, we recall that any interaction between the bosons should lead to thermal equilibrium and in the case of large occupation numbers to the formation of a Bose-Einstein condensate. Gravitational interaction is not an exception, as pioneering works [11,16] argued. But then the condensate cannot appear in a homogeneous state [17]. Rather, it should fragment due to Jeans instability into a set of isolated Bose stars (cf. [8]), which is therefore the actual end state of the condensation process.

The field profiles of the isolated Bose stars are found by solving Eqs. (2) with the stationary spherical ansatz $\psi = \psi_s(r) e^{-i\omega_s t}$, $U = U_s(r)$ at each $\omega_s < 0$; see, e.g., [22]. We computed them using a separate code. Results coincide with the profiles of condensed objects on the lattice [see Fig. 1(c)], thus proving that we indeed observe the nucleation of Bose stars. We performed simulations for a large set of parameters, for δ- and θ-like initial distributions, $|\psi_{\boldsymbol{p}}|^2 \propto \delta(|\boldsymbol{p}| - mv_0)$ and $\theta(mv_0 - |\boldsymbol{p}|)$, in addition to the Gaussian. Every time, we observed the formation of a Bose star with correct profile $\psi_s(r)$, $U_s(r)$ correct mass $M_s \propto \psi_s^{1/2}(0)$, and correct size proportional to M_s^{-1}; see [22]. Note that the Bose stars nucleate wide and rarefied, then shrink, and become dense as they accumulate bosons. Unlike in other studies, no "seed" Bose condensate was present in our simulations at $\tau < \tau_{gr}$; otherwise, it would grow above the background in a short time—see Fig. 1(d).

The spectrum.—To look deeper into the initial, seemingly featureless stage of gas evolution, we compute the distribution $F(t, \omega) = dN/d\omega$ of bosons over energies ω. This quantity equals the Fourier image of the correlator

$$F = \int \frac{dt_1}{2\pi} d^3\boldsymbol{x} \psi^*(t, \boldsymbol{x}) \psi(t + t_1, \boldsymbol{x}) e^{i\omega t_1 - t_1^2/\tau_1^2} \qquad (3)$$

in the kinetic regime $(mv_0^2)^{-1} \ll \tau_1 \ll \tau_{gr}$; see Supplemental Material Sec. S1 [19] and Ref. [23]. In dimensionless calculations, we use $\tilde{F} = mv_0^2 F/N$ normalized to unity: $\int \tilde{F} d\tilde{\omega} = 1$, where $\tilde{\omega} = \omega / mv_0^2$.

Figure 1(e) shows that the spectrum (3) completely changes during evolution at $t < \tau_{gr}$. It starts from a wide bell $\tilde{F} \propto \tilde{\omega}^{1/2} e^{-2\tilde{\omega}}$ corresponding to Gaussian distribution in momenta in Fig. 1(a). As time goes on, F develops a peak at low ω and becomes close to thermal at intermediate energies, $F \propto \omega^{-1/2}$; see the graph at $t \sim \tau_{gr}$ in Figs. 1(e) and 1(f). At high ω, it still falls off exponentially, as high-frequency modes thermalize slowly [24]. Once the Bose star nucleates, a small δ peak appears in the distribution. With time, this δ peak grows in height and shifts to the left; see the spectrum 1b in Fig. 1(e). It explicitly shows condensed particles of the same energy $\omega_s < 0$ inside the growing Bose star.

Below, we use the δ peak at $\omega < 0$ as an indicator of Bose star nucleation: We define τ_{gr} as the moment when the peak is twice higher than the fluctuations in $F(t, \omega)$.

Condensation time.—In the kinetic regime, evolution of $F(t, \omega)$ is described by a kinetic equation—this fact can be proven by solving Eqs. (2) perturbatively and using approximations (1); see Supplemental Material Sec. S1 [19] and cf. Refs. [23,25]. One therefore expects that the time of Bose star formation τ_{gr} is proportional with some coefficient b to the kinetic relaxation time: $\tau_{gr} = 4b\sqrt{2}/(\sigma_{gr} v n f)$, where $\sigma_{gr} \approx 8\pi (mG)^2 \Lambda / v^4$ is the transport Rutherford cross

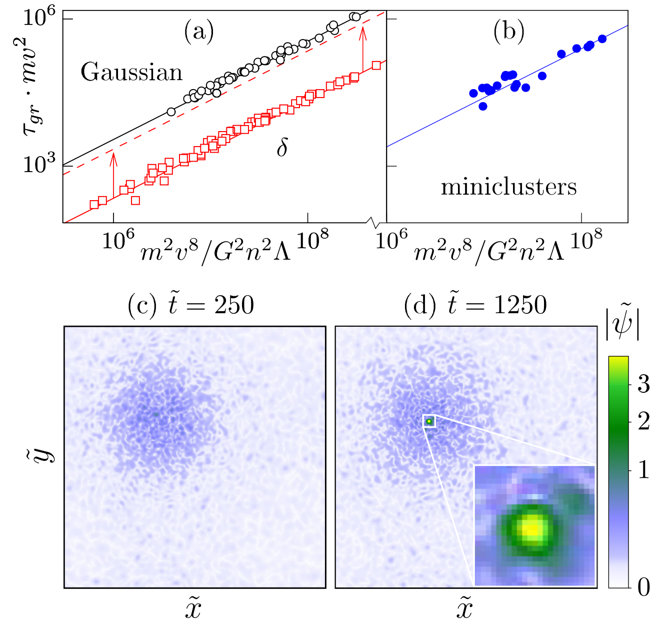

FIG. 2. (a) Time to Bose star formation in the cases of Gaussian (empty circle) and δ-peaked (empty square) initial distributions. The δ graphs are shifted downwards ($\tau_{gr} \to \tau_{gr}/10$) for visualization purposes. Lines depict fits by Eq. (4). (b) The same for isolated miniclusters. (c),(d) Slices $\tilde{z} = \text{const}$ of the solution $|\tilde{\psi}(\tilde{t}, \tilde{\boldsymbol{x}})|$ describing the formation of a Bose star in the center of a minicluster; $\tilde{N} = 290$, $\tilde{L} \approx 63$.

section of gravitational scattering, $\Lambda = \log(mvL)$ is the Coulomb logarithm, and $f = 6\pi^2 n/(mv)^3 \gg 1$ is the phase-space density that appears due to Bose stimulation [8]. The coefficient $b = O(1)$ accounts for the details of the process. It is expected to depend weakly on the initial distribution.

Taking all factors together, we obtain the expression

$$\tau_{gr} = \frac{b\sqrt{2}}{12\pi^3} \frac{mv^6}{G^2 n^2 \Lambda}, \qquad b \sim 1, \tag{4}$$

that apart from the Coulomb logarithm Λ involves only local parameters, i.e., the boson number density n and characteristic velocity v. So, up to weak logarithmic dependence on the size L, the formation of the Bose star can be regarded as a local process, with a periodic box representing a central part of some DM halo. We will confirm this intuition below.

We performed simulations of the gas with a Gaussian initial distribution at different $\tilde{L}$ and $\tilde{n}$. Our results for τ_{gr} [circles in Fig. 2(a)] cover 2 orders of magnitude, but they are nevertheless well fitted by Eq. (4) with $v = v_0$ and $b \approx 0.9$ [upper line in Fig. 2(a)]. To confirm that Eq. (4) is universal, we repeated the calculations for the initial δ distribution, $|\psi_{\boldsymbol{p}}|^2 \propto \delta(|\boldsymbol{p}| - mv_0)$ [squares in Fig. 2(a)]. The new vales of τ_{gr} are still described by Eq. (4), albeit with slightly different coefficient $b \approx 0.6$. We conclude that Eq. (4) is a practical and justified expression for the time of Bose star formation.

Kinetics.—Let us show that the evolution of $F(t, \omega)$ in Fig. 1(e) is indeed governed by the Landau kinetic equation [24] for the homogeneous isotropic Coulomb ensemble:

$$\partial_t \tilde{F} = \tau_0^{-1} \partial_{\tilde{\omega}} [\tilde{A} \partial_{\tilde{\omega}} \tilde{F} + (\tilde{B}\, \tilde{F} - \tilde{A}) \tilde{F}/2\tilde{\omega}]; \tag{5}$$

see Supplemental Material Sec. S1 4 [19] for a derivation. Here the scattering integral in the right-hand side involves $\tilde{A}(\tilde{\omega}) = \int_0^\infty d\tilde{\omega}_1 \min^{3/2}(\tilde{\omega}, \tilde{\omega}_1) \tilde{F}^2(\tilde{\omega}_1)/(3\tilde{\omega}_1 \tilde{\omega}^{1/2})$ and $\tilde{B}(\tilde{\omega}) = \int_0^{\tilde{\omega}} d\tilde{\omega}_1 \tilde{F}(\tilde{\omega}_1)$, and it is explicitly proportional to the inverse relaxation time $\tau_0^{-1} = 8\pi^3 n^2 G^2 (\Lambda + a)/mv_0^6 \sim \tau_{gr}^{-1}$. Notably, Eq. (5) is valid in the leading logarithmic approximation $\Lambda \gg 1$, which is too rough for our numerical solutions with $\Lambda \sim 5$. To get a quantitative comparison, we added an unknown correction $a = O(1)$ to Λ.

We numerically evolve Eq. (5) starting from the same initial distribution as in Fig. 1. In Fig. 1(f), the solution $F(t, \omega)$ (circles) is compared to the microscopic distribution (3) (dashed line) at $t \approx \tau_{gr}$, where $a \approx 5$ is obtained from the fit. We observe an agreement in the kinetic region $\tilde{\omega} \gg 2\pi^2/\tilde{L}^2$, which confirms Eq. (5) at $t < \tau_{gr}$.

Note that, unlike in the case of short-range interactions [26], thermalization in the Landau equation does not proceed via power-law turbulent cascades [24], and we do not observe them in Figs. 1(e) and 1(f). Nevertheless, we think that Eq. (5) provides the basis for an analytic description of gravitational Bose-Einstein condensation.

Miniclusters.—So far, we have assumed that a homogeneous ensemble in the box correctly describes central parts of DM halos. Now, we study the isolated halos themselves and verify this assumption. Recall that in a large volume nonrelativistic gas forms clumps at scales $R \gtrsim 2\pi/k_J$ due to Jeans instability, where $k_J^2 = 2\pi G n m^2 \langle \omega^{-1} \rangle$ and the average is computed with $F(\omega)$. Starting numerical evolution from the homogeneous ensemble with δ-distributed momenta at $L > 2\pi/k_J$, we indeed observe the formation of a virialized minicluster in Fig. 2(c). With time, it remains stationary until the Bose star appears in its center; see Fig. 2(d) and movie [19]. Thus, the formation of Bose stars is not specific to finite boxes.

We checked that our kinetic expression for τ_{gr} works for the virialized miniclusters. To this end, we generated many different miniclusters, computed their central densities n and virial velocities $\langle v^2 \rangle = -2\langle \omega \rangle / m$ using the $\omega < 0$ part of the distribution $F(\omega)$, and estimated their radii R. In Fig. 2(b), we plot the times of Bose star formation in the miniclusters versus these parameters and $\Lambda = \log(mvR)$ (points). The numerical data are well approximated by Eq. (4) with $b \approx 0.7$ (line), although the statistical fluctuations are now larger due to limited control over the momentum distribution inside the miniclusters.

Estimating the virial velocity $v^2 \sim 4\pi GmnR^2/3$ in the halo of radius R, one recasts Eq. (4) in the intuitively simple form $\tau_{gr} \sim 0.047(R/v)(Rmv)^3/\Lambda$, where the numerical factor is computed. Remarkably, τ_{gr} equals to the free-fall time R/v multiplied by the cube of kinetic constant $Rmv \gg 1$ in Eq. (1). In the nonkinetic case $Rmv \sim 1$, the Bose stars form immediately [12,13,15].

Bose star growth.—After nucleation, the Bose stars start to acquire particles from the ensemble. Because of computational limitations, we are able to observe only the first decade of their mass increase that proceeds according to the heuristic law $M_s(t) \simeq cv_0(t/\tau_{gr} - 1)^{1/2}/Gm$ with $c = 3 \pm 0.7$. The ratio t/τ_{gr} in this expression suggests that the growth of the Bose stars is a kinetic process deserving a separate study.

Discussion.—Let us argue that the Bose stars appear in the popular cosmological models even if we conservatively assume that halos or miniclusters in these models are initially virialized. If the DM is made of invisible QCD axions [3], the smallest substructures are axion miniclusters [27,28] of typical mass $M_c \sim 10^{-13}\ M_\odot$ [29]. These miniclusters can be characterized [28] by the ratio $\Phi + 1 \equiv n/\bar{n}|_{RD}$ of their central density n to the cosmological axion density $\bar{n}$ at the radiation-dominated stage when they are still in the linear regime. Substituting their typical parameters [28] into Eq. (4) and expressing the result in terms of Φ and M_c, we find

$$\tau_{gr} \sim \frac{10^9\ \mathrm{yr}}{\Phi^3(1+\Phi)} \left(\frac{M_c}{10^{-13}\ M_\odot}\right)^2 \left(\frac{m}{26\ \mu\mathrm{eV}}\right)^3,$$

where the reference axion mass is taken from Ref. [9]. Thus, typical miniclusters with $\Phi \sim 1$ condense during the lifetime of the Universe, the densest ones with $\Phi \sim 10^3$ [28] in several hours. Bose stars are important [6], as they hide a part of DM from observations. After becoming large, they may explode into relativistic axions [7] or emit radiophotons via parametric resonance [2], which at different redshifts may explain FRBs [30] and the anomalies of ARCADE 2 and EDGES [31].

Note that the gravitational relaxation of virialized QCD axions is significantly faster than the relaxation due to self-coupling $\lambda \equiv m^2/f_a^2$, where $f_a \sim 10^{11}$ GeV is the Peccei-Quinn scale. Indeed, in the kinetic regime the relaxation rates are proportional to the cross sections, and $\tau_{\mathrm{self}}/\tau_{gr} \sim \sigma_{gr}/\sigma_{\mathrm{self}} \sim (10 f_a G^{1/2}/v)^4$. In typical miniclusters $v \sim 10^{-10} \ll 10 f_a G^{1/2}$, and gravitational interactions win by $\tau_{\mathrm{self}}/\tau_{gr} \sim 10^{12}$.

Another popular class of DM models is based on string axions forming fuzzy DM [4]. An interesting though recently constrained [32] scenario considers the smallest mass $m \sim 10^{-22}$ eV of these particles [15] when their de Broglie wavelength inside the dwarf galaxies is comparable to the size of the galaxy cores, $mvR \sim 1$. As we argued, the Bose stars should appear in these cores in free-fall time. This explains their fast formation [15] in numerical simulations. At larger masses, one substitutes typical parameters of dwarf satellites into Eq. (4):

$$\tau_{gr} \sim 10^6\ \mathrm{yr} \left(\frac{m}{10^{-22}\ \mathrm{eV}}\right)^3 \left(\frac{v}{30\ \mathrm{km/s}}\right)^6 \left(\frac{0.1\ M_\odot/\mathrm{pc}^3}{\rho}\right)^2.$$

The Bose stars nucleate there if $m \lesssim 2 \times 10^{-21}$ eV, at the boundary of an experimentally allowed mass window [32]. Then the missing satellites may hide as Bose stars. At even larger m, the Bose stars may form in miniclusters and in cores of large galaxies. They may also grow overcritical and explode [7]. Note that self-interaction of typical string axions [10] with $f_a \sim 10^{-2} G^{-1/2}$ is less effective than gravity, because $v \ll 10 f_a G^{1/2}$ in all structures.

We thank A. Pustynnikov, D. Gorbunov, M. Ivanov, E. Nugaev, and V. Rubakov for discussions. This work was supported by Grant No. RSF 16-12-10494. Numerical calculations were performed on the Computational cluster of TD INR RAS.

*levkov@ms2.inr.ac.ru

[1] R. Ruffini and S. Bonazzola, Phys. Rev. **187**, 1767 (1969).
[2] I. I. Tkachev, Sov. Astron. Lett. **12**, 305 (1986).
[3] P. Sikivie, Lect. Notes Phys. **741**, 19 (2008).
[4] A. Ringwald, Phys. Dark Universe **1**, 116 (2012).
[5] F. E. Schunck and E. W. Mielke, Classical Quantum Gravity **20**, R301 (2003).
[6] J. Eby, M. Leembruggen, P. Suranyi, and L. C. R. Wijewardhana, J. High Energy Phys. 12 (2016) 066; P. S. B. Dev, M. Lindner, and S. Ohmer, Phys. Lett. B **773**, 219 (2017); T. Helfer *et al.*, J. Cosmol. Atropart. Phys. 03 (**2017**) 055; J. Eby, M. Leembruggen, J. Leeney, P. Suranyi, and L. C. R. Wijewardhana, J. High Energy Phys. 04 (2017) 099; E. Braaten, A. Mohapatra, and H. Zhang, Phys. Rev. D **96**, 031901 (2017); P.-H. Chavanis, Phys. Rev. D **98**, 023009 (2018); L. Visinelli, S. Baum, J. Redondo, K. Freese, and F. Wilczek, Phys. Lett. B **777**, 64 (2018).
[7] D. G. Levkov, A. G. Panin, and I. I. Tkachev, Phys. Rev. Lett. **118**, 011301 (2017).
[8] I. I. Tkachev, Phys. Lett. B **261**, 289 (1991); S. Khlebnikov and I. Tkachev, Phys. Rev. D **61**, 083517 (2000).
[9] V. B. Klaer and G. D. Moore, J. Cosmol. Astropart. Phys. 11 (2017) 049.
[10] A. Arvanitaki, S. Dimopoulos, S. Dubovsky, N. Kaloper, and J. March-Russell, Phys. Rev. D **81**, 123530 (2010).
[11] P. Sikivie and Q. Yang, Phys. Rev. Lett. **103**, 111301 (2009); O. Erken, P. Sikivie, H. Tam, and Q. Yang, Phys. Rev. D **85**, 063520 (2012).
[12] E. Seidel and W.-M. Suen, Phys. Rev. Lett. **72**, 2516 (1994); F. S. Guzman and L. A. Urena-Lopez, Astrophys. J. **645**, 814 (2006).
[13] H.-Y. Schive, M. H. Liao, T. P. Woo, S. K. Wong, T. Chiueh, T. Broadhurst, and W. Y. Pauchy Hwang, Phys. Rev. Lett. **113**, 261302 (2014).

[14] B. Schwabe, J. C. Niemeyer, and J. F. Engels, Phys. Rev. D **94**, 043513 (2016); M. Bezares, C. Palenzuela, and C. Bona, Phys. Rev. D **95**, 124005 (2017).
[15] H.-Y. Schive, T. Chiueh, and T. Broadhurst, Nat. Phys. **10**, 496 (2014).
[16] S. Khlebnikov, Phys. Rev. D **62**, 043519 (2000).
[17] A. H. Guth, M. P. Hertzberg, and C. Prescod-Weinstein, Phys. Rev. D **92**, 103513 (2015).
[18] S. Y. Khlebnikov and I. I. Tkachev, Phys. Rev. Lett. **77**, 219 (1996).
[19] See Supplemental Material at http://link.aps.org/supplemental/10.1103/PhysRevLett.121.151301 for the derivation of kinetic equation (Sec. S1), details of numerical method (Sec. S2,), and two movies demonstrating gravitational Bose-Einstein condensation in the box and in minicluster.
[20] H. Yoshida, Phys. Lett. A **150**, 262 (1990).
[21] http://docs.nvidia.com/cuda/cufft/index.html.
[22] P.-H. Chavanis, Phys. Rev. D **84**, 043531 (2011).
[23] V. Zakharov, V. L'vov, and G. Falkovich, *Kolmogorov Spectra of Turbulence I. Wave Turbulence* (Springer, Berlin, 1992).
[24] V. E. Zakharov and V. I. Karas, Phys. Usp. **56**, 49 (2013).
[25] E. M. Lifshitz and L. P. Pitaevskii, *Physical Kinetics*, Course on Theoretical Physics Vol. 10 (Pergamon, New York, 1981).
[26] D. V. Semikoz and I. I. Tkachev, Phys. Rev. Lett. **74**, 3093 (1995); Phys. Rev. D **55**, 489 (1997).
[27] C. J. Hogan and M. J. Rees, Phys. Lett. B **205**, 228 (1988).
[28] E. W. Kolb and I. I. Tkachev, Phys. Rev. Lett. **71**, 3051 (1993); Phys. Rev. D **49**, 5040 (1994); Astrophys. J. **460**, L25 (1996).
[29] J. Enander, A. Pargner, and T. Schwetz, J. Cosmol. Astropart. Phys. 12 (2017) 038.
[30] I. I. Tkachev, JETP Lett. **101**, 1 (2015).
[31] J. Kehayias, T. W. Kephart, and T. J. Weiler, J. Cosmol. Astropart. Phys. 10 (2015) 053; S. Fraser *et al.*, Phys. Lett. B **785**, 159 (2018).
[32] V. Iršič, M. Viel, M. G. Haehnelt, J. S. Bolton, and G. D. Becker, Phys. Rev. Lett. **119**, 031302 (2017); E. Armengaud, N. Palanque-Delabrouille, C. Yèche, D. J. E. Marsh, and J. Baur, Mon. Not. R. Astron. Soc. **471**, 4606 (2017).